Reverse-time migration imaging with/without multiples

Zaiming Jiang, John C. Bancroft, and Laurence R. Lines

ABSTRACT

One of the challenges with reverse-time migration based on finite-difference method is the problems of computational costs, in terms of free disk space and/or computational time. This report discusses the principle of a new imaging condition, referred as 'first arrival imaging condition', and shows the advantage of less computational costs of this method, compared to the widely used source-normalized crosscorrelation imaging condition for reverse-time migration.

Principally, with crosscorrelation imaging conditions, all the multiples inside both forward modelling and reverse-time migration wavefields are involved; on the other hand, with the first arrival imaging condition, the multiples in the wavefields are not included.

INTRODUCTION

Finite-difference modelling and reverse-time migration based on finite-difference methods are compute-intensive. One challenge is the long computational time, and another is the requirement of huge disk space. The two problems are linked to each other.

Modelling and reverse-time migration are both time consuming. Finite-difference Elastic wave modelling itself needs very long computational time. For example, it took Martin (2004) a total of 70,000 hours, or approximately 8 CPU years to do elastic wave modelling using the Marmousi2 model. Prestack reverse-time migration needs even longer computational time. People (Gavrilov, Lines, Bland, and Kocurko, 2000; Jiang, Bonham, Bancroft, and Lines, 2010) have already practiced parallel computing to accelerate reverse-time migration.

The popular crosscorrelation imaging conditions (Claerbout, 1971; Whitmore and Lines, 1986; Kaelin and Guitton, 2006; Chattopadhyay and McMechan, 2008) require huge disk space. Jiang, Bonham, Bancroft, and Lines (2010) have addressed this problem and provided a solution by doing the modelling part of reverse-time migration twice, instead of once, to reduce this disk space problem at the cost of additional computational time.

This report suggests a new imaging condition. The imaging condition depends on the extraction of first arrival amplitudes and times from the forward modelling wavefields, so it is referred as 'first arrival imaging condition'. With this imaging condition, the requirement of computational resources, in terms of CPU cycles and free disk space, is reduced, compared to crosscorrelation imaging conditions.

Thus, this report will (1) review the details of our reverse-time migration implementation, which is based on a staggered-grid finite-difference method, (2) review the principle of crosscorrelation imaging conditions, and show the experimental results using a point diffractor subsurface model and a reduced set of Marmousi2 models, (3) address the principle of first arrival imaging condition, show the results, and discuss the pros and cons.

REVERSE-TIME MIGRATION

The procedures of a reverse-time migration algorithm include three parts: forward modelling, reverse-time extrapolation, and imaging. Both the forward modelling and reverse-time extrapolation involve a finite-difference algorithm. The finite-difference method used in our forward modelling and reverse-time migration is based on a staggered-grid scheme with velocity/stress and time splitting, which was first presented by Virieux (1986).

Forward modelling

One gets the "downgoing wave" from the forward modelling. The input of the forward modelling is a subsurface model. In our case of staggered-grid scheme, a subsurface model consists of three parameter sets: two parameter sets of Lame coefficients and one set of densities. Or equivalently, the three parameter sets are P-wave velocities, S-wave velocities, and densities.

In addition to the finite-difference scheme, the modelling algorithm involves the implementation of (1) seismic sources, (2) free surface boundary conditions, and (3) computational boundary conditions.

The seismic sources are explosive sources. An explosive source consists of four zero phase Ricker wavelets with peak frequency equal to 40 Hz. The source scheme is explained by Manning (2008) in detail.

The free surface boundary conditions are the stresses on the surface must be zero.

The implementation of the computational boundary conditions in our experiment is a method combining the absorbing boundary conditions (Engquist and Majda, 1977; Clayton and Engquist, 1977) and the nonreflecting boundary condition (Cerjan, Kosloff, Kosloff, and Reshef, 1985). The method is explained in detail by Jiang, Bancroft, and Lines (2010).

Reverse-time extrapolation

One gets the "upgoing wave" from the reverse-time extrapolation. The input of reverse-time extrapolation is a subsurface model, which is the same as for the forward modelling, and recorded seismic data from the surface. In our experiments, the recorded data on the surface are the vertical and horizontal components. In the case of numerical experiments, the surface recorded data are from the forward modelling.

Before the actual reverse-time extrapolation, the surface records needs to be preprocessed. The preprocessing mainly includes (1) direct wave muting and (2) surface wave removal. The preprocessed surface records consist of only reflections from subsurface reflectors, ideally.

The preprocessed surface records are extrapolated by the same finite-difference method as for the forward modelling. However, the extrapolation is in reverse-time. Also, there are no explosive sources involved. Instead, the preprocessed surface records are fed on the surface in reverse-time.

Imaging

The procedure of imaging is to find positions and reflection strengths of existing subsurface reflectors.

People in the literature are curious about the effects of multiples in reverse-time migration. On one hand, what if we image with all the multiples? On the other hand, what if we image without the multiples? And how could we suppress the multiples?

The normalized crosscorrelation imaging condition is one imaging method with all the multiples. People have developed a few imaging conditions and the normalized crosscorrelation imaging condition is one of the preferred methods for reverse-time migration (Chattopadhyay and McMechan, 2008). The section titled "imaging with multiples" will show the result of the normalized crosscorrelation imaging condition. We will show that all the multiples are involved in this method.

We tried out another imaging condition, inspired by the work done by Loewenthal and Hu (1991). "Reflectors exist at points in the ground where the first arrival of downgoing wave is time coincide with an upgoing wave" (Claerbout, 1971) . By extracting the first arrivals of the downgoing wave, an imaging condition without any multiples in the snapshots for imaging is implemented. This is shown in the section of "imaging without multiples".

IMAGING WITH MULTIPLES

(This secion is partly from a paper by Jiang, Bancroft, Lines, and Hall in 2010.)

Source-normalized crosscorrelation imaging condition (Claerbout, 1971; Whitmore and Lines, 1986; Kaelin and Guitton, 2006; Chattopadhyay and McMechan, 2008) is

$$image(x,z) = \frac{\sum_{time} S(x,z,t)R(x,z,t)}{\sum_{time} S^2(x,z,t)} \qquad (1)$$

where *S(x,z,t)* and *R(x,z,t)* are, respectively, the source wavefield produced by forward modelling and the receiver wavefield produced by reverse-time extrapolation; *S(x,z,t)R(x,z,t)* at certain time is interpreted as the coherence of the forward modelling wavefield and the reverse-time wavefield.

For a subsurface model of a homogeneous medium contains a point diffractor, shown in Figure 1, the forward modelling snapshots, the reverse-time extrapolation snapshots, and the crosscorrelations of both wavefields are shown in Figure 2.

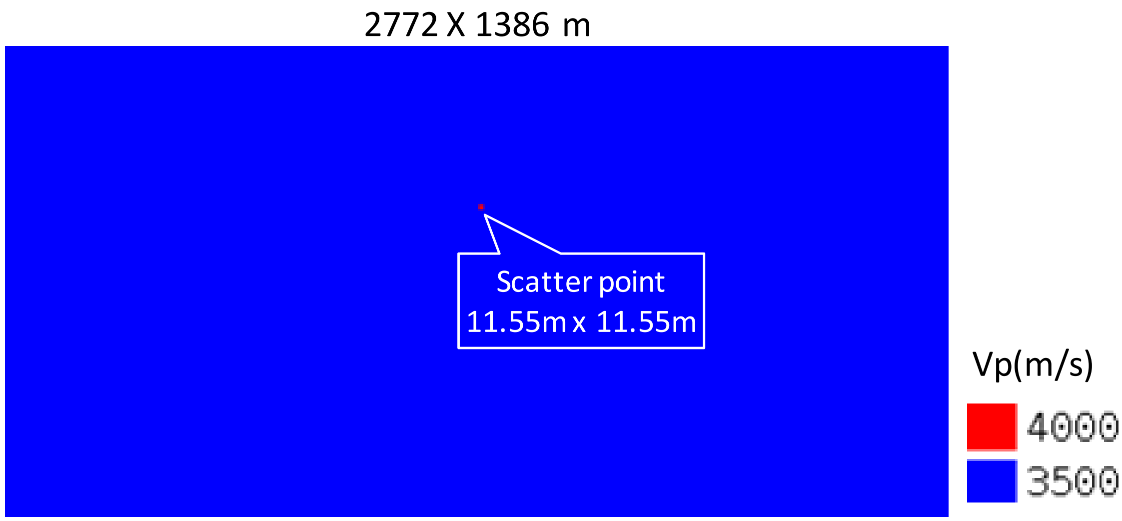

FIG. 1. A subsurface model of a homogeneous medium containing a point diffractor. Here only P-wave velocities are shown (After Jiang, Bancroft, Lines, and Hall, 2010).

The snapshots at different times from both source and receiver wave fields are used when applying source-normalized crosscorrelation imaging condition. All the snapshots include both primary arrivals and multiples.

For a reduced set of Marmousi2 model, shown as the top picture in Figure 3, the result of reverse-time migration is shown as the bottom picture in Figure 3.

The multiples in both forward modelling and reverse-time migration wavefileds will cause very low frequency artifacts in the stacked imaging results. The artifacts can be reduced to a very low level by applying a high-pass filter (Jiang, Bancroft, Lines, and Hall, 2010).

Thus, the general steps of imaging include (1) calculation of crosscorrelation of source wavefield from forward modelling and receiver wavefield from reverse-time extrapolation, shot by shot, resulting in shot images, (2) stacking of the shot images, (3) application of high pass filters to reduce the very low frequency artifacts.

The challenges coming with this imaging condition are the computational cost problems. The problems and the solutions are described by Jiang, Bonham, Bancroft, and Lines in 2010.

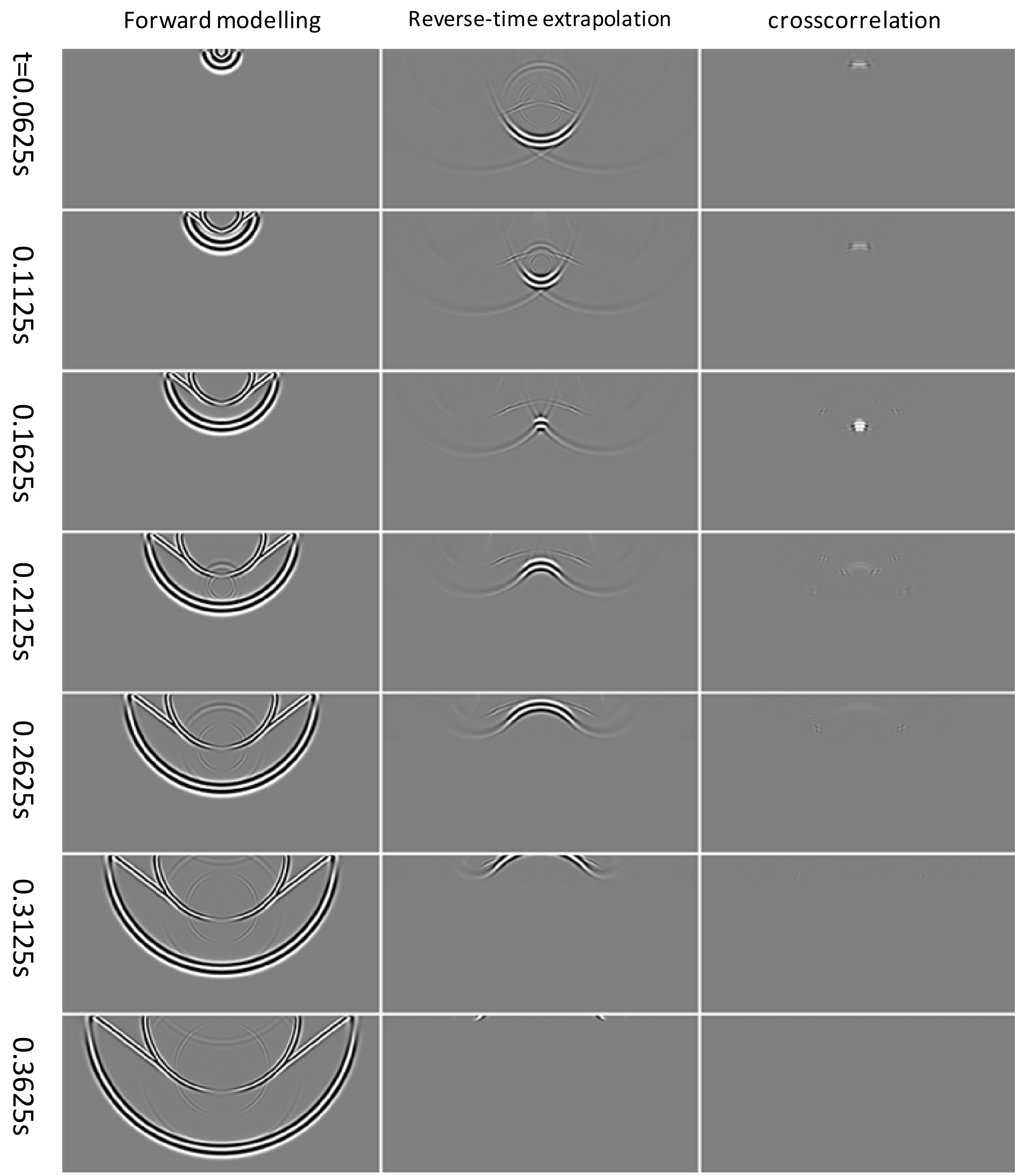

FIG. 2. Source-normalized crosscorrelation imaging condition. (After Jiang, Bancroft, Lines, and Hall, 2009)

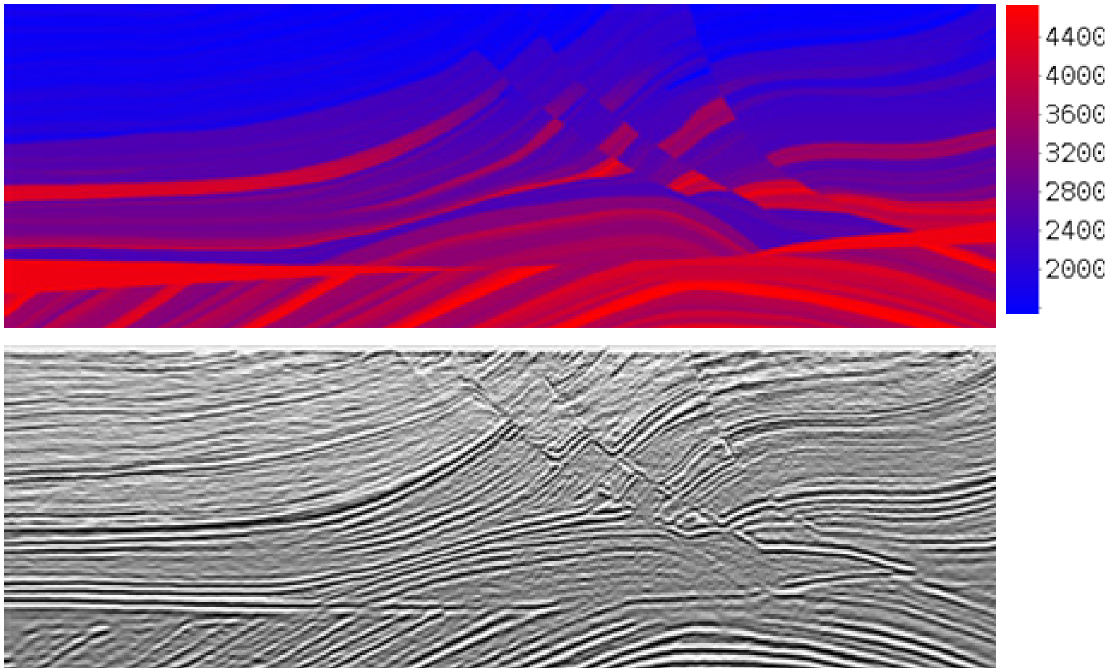

FIG. 3. A reduced set of Marmousi2 and the result of reverse-time migration by source normalized crosscorrelation imaging condition. The result is from 64 shots.

IMAGING WITHOUT MULTIPLES

This section shows a different imaging condition from the one in the last section. By extracting the first arrivals of the downgoing waves, an imaging condition without any multiples in the snapshots for imaging is implemented. This method, compared to the crosscorrelation imaging condition, needs neither huge disk space nor additional computational time.

Extracting first arrivals of the downgoing wave

When an explosive seismic source is placed on the surface, the generated waves include P wave, S wave, downgoing head waves, and surface waves. On surface part of the earth (or subsurface model, in the case of numerical modelling), the strongest energy is the surface waves. Deeper inside the earth, it is assumed that the strongest seismic vibration is within the P-wave wave front.

We use two criteria to extract first arrivals of the downgoing waves.

The first is maximum amplitudes. Deep inside the earth, the strongest energy is within the P-wave wave front, so it is reasonable to extract the first arrivals by the maximum amplitude criteria.

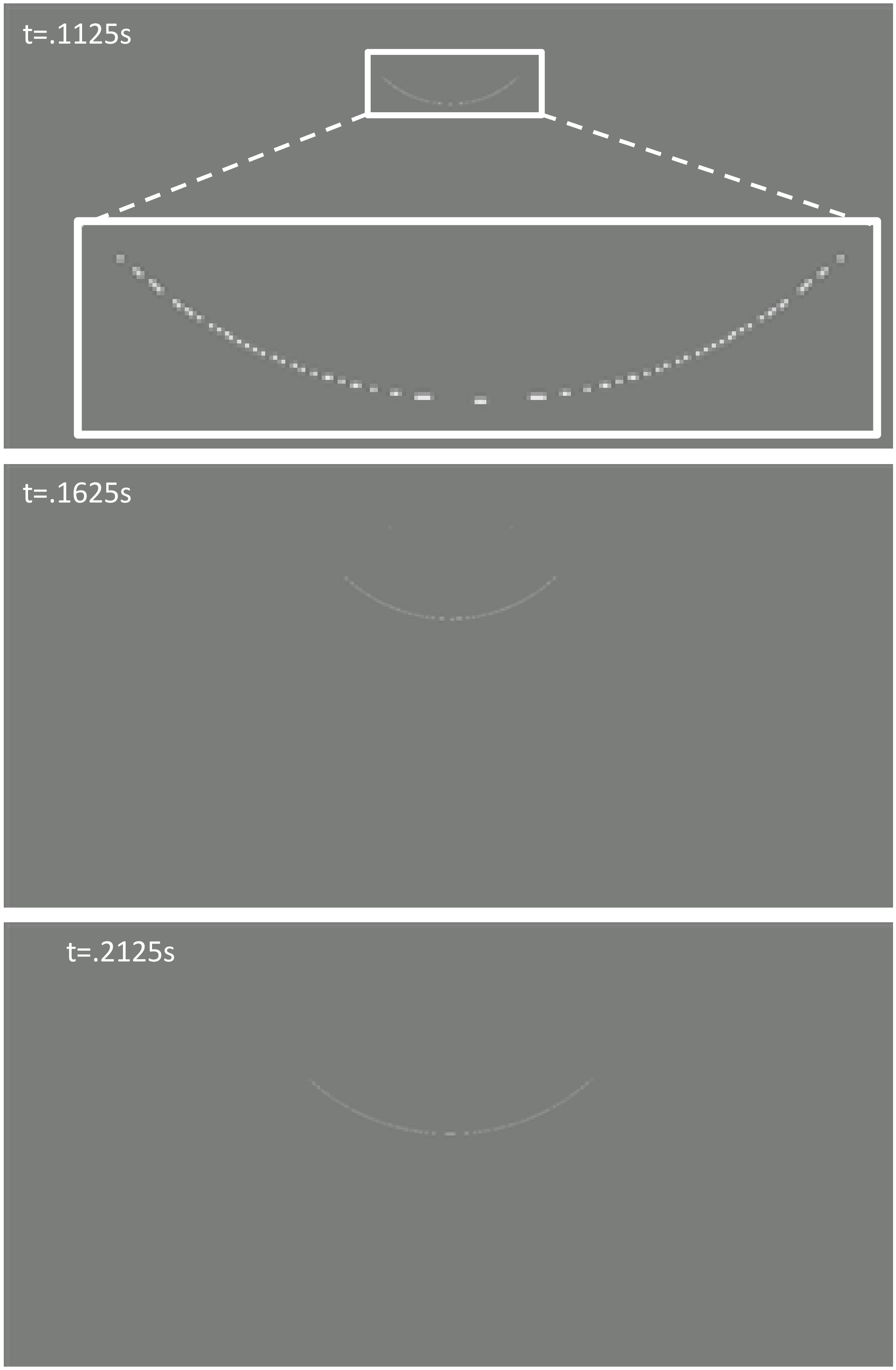

FIG. 4. First arrivals of the downgoing wave at five different times. The subsurface model is the same as defined in Figure 1. The big box is a zoom of the small box.

The second criterion is minimum times. When the wave traveling inside the part close to earth surface, a particle at one point will vibrate four times: the first one is caused by the P wave arrival, the second is by the downgoing headwave arrival, the third is by the S-wave arrival, and the fourth is by the surface wave. The surface wave, which is the slowest and comes outwards with maximum time, could be stronger than any of the P-wave, the downgoing headwave, and the S-wave. If we extract only by the maximum amplitude criterion, we might get wrong first arrival times for the points close to the earth surface. Thus, we also use the minimum time criterion, along with the maximum amplitude criterion, to extract the first arrivals. In practice, we use an amplitude threshold to recognize the arrival of P-wave, which has the minimum time, and thus reject the times of maximum amplitude of surface waves.

For each point on the earth subsurface (each node of the subsurface model in numerical modelling) of one shot gather processing, there are two values are required to be stored for imaging purpose: one is the first arrival amplitude across this specific point, and the other is the first arrival time. The First arrivals of the downgoing wave at different times for the point diffractor subsurface model, shown in Figure 1, are shown in Figure 4. Here only a pie slice of 90 degrees under the source is extracted.

Imaging

For each point inside the subsurface, the image is determined by only the time of first arrivals of downgoing waves, which are different from the crosscorrelation imaging conditions. At this specific time of first arrival of downgoing wave, the image is calculated by

$$image(x, z, first\ arrival\ time) = \frac{R(x,z,first\ arrival\ time)}{S(x,z,first\ arrival\ time)}. \tag{2}$$

This imaging condition depends on the extracting of first arrivals from the downgoing wavefields. For reference, we call it ‘first arrival imaging condition’.

At time 0.1625s, for the pointer diffractor subsurface model, the image snapshot is shown in Figure 5. The image snapshots at times close to this specific time are similar, indicating the existence of the point diffractor; but the image snapshots at other times show almost nothing, since there are no other reflectors in the subsurface model causing reflections or refractions.

For the reduced set of Marmousi2 model shown in Figure 3, the result of reverse-time migration by the new imaging condition is shown in Figure 6. Compared to the result shown in Figure 3, there exist stronger imaging artifacts at the part close the surface.

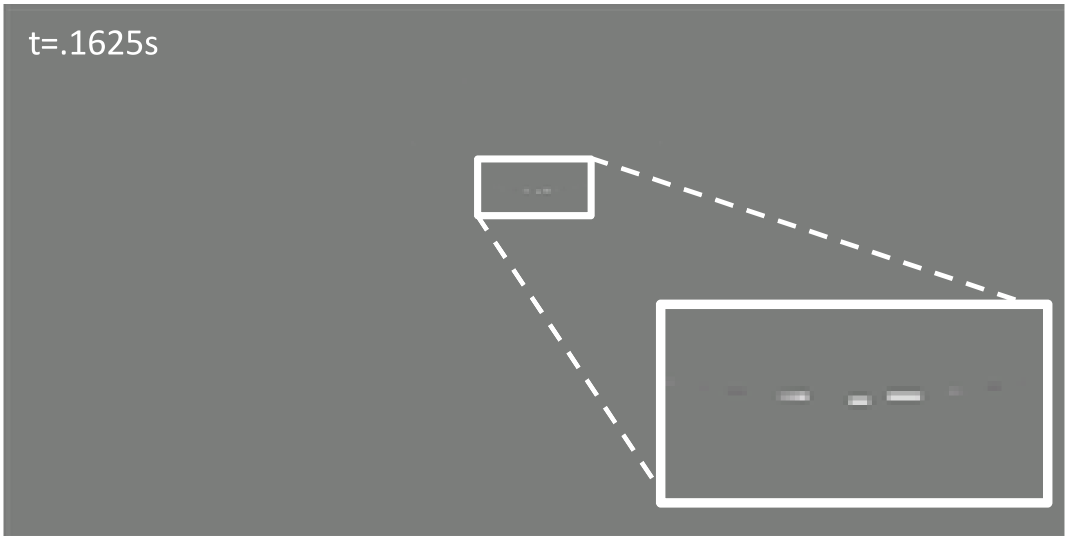

FIG. 5. Imaging snapshot at the time close to the real first arrival time. The subsurface model is the same as defined in Figure 1. The big box is a zoom of the small box.

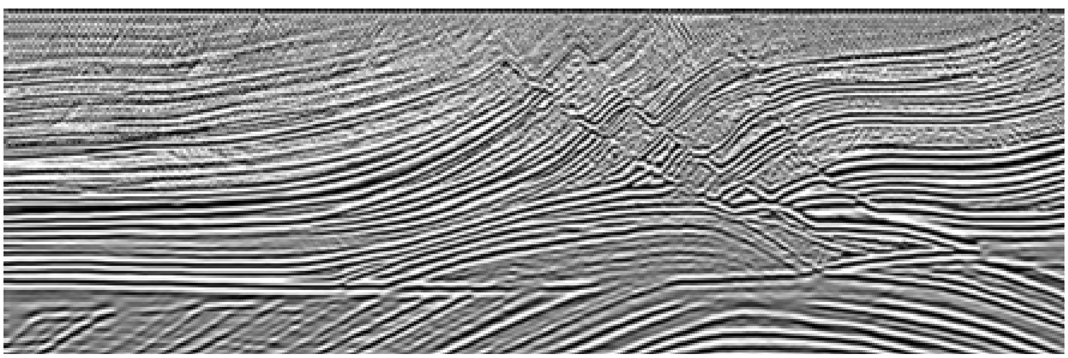

FIG. 6. Imaging result of a reduced set of Marmousi2 model by the reverse-time migration with first arrival imaging condition. This is from 256 shots.

Advantages

There are huge advantages of the first arrival imaging condition compared to crosscorrelation imaging conditions, in terms of computational costs. As stated by Jiang, Bonham, Bancroft, and Lines in 2010, the crosscorrelation imaging condition requires huge disk space to store the snapshots of forward modelling, and a method of modelling twice was designed to overcome this problem. This leads to longer processing time. And the need to do disk I/O makes the situation worse, since disk I/O is much slower than calculation in memory. On the other hand, with the first arrival imaging condition, for each point only two values, the first arrival amplitude and the first arrival time, are required to be stored. Thus, there is neither the problem of huge disk space requirement nor the problem of additional modelling time.

We compared the computational time of the two imaging methods. The computational times of reverse-time migration using source normalized crosscorrelation imaging condition and first arrival imaging condition are estimated to be 2.5:1.

CONCLUSIONS

By maximum amplitude and minimum time criteria, first arrivals in the subsurface are extracted as the downgoing wave, then the data are used in first arrival imaging condition.

The first arrival imaging condition requires much less free disk space for the store of forward modelling wavefield, compared to the crosscorrelation imaging conditions, for which the requirement of huge disk space leads to additional computational time for large subsurface models.

The first arrival imaging condition presented in this report needs to be optimized to reduce the imaging artifacts in the shallow part of the subsurface.

ACKNOWLEDGEMENTS

We thank the sponsors of CREWES for their continued support.

REFERENCES

Cerjan, C., Kosloff, D., Kosloff, R., and Reshef, M, 1985, A nonreflecting boundary condition for discrete acoustic and elastic wave equations, Geophysics, **50**, 705-708.

Chattopadhyay, S., and McMechan, G.A., 2008, Imaging conditions for prestack reverse-timemigration: Geophysics, **73**, no. 3, S81–S89.

Claerbout, J. F., 1971, Toward a unified theory of reflector mapping: Geophysics, **36**, 467–481.

Clayton, R., and Engquist, B., 1977, Absorbing boundary conditions for acoustic and elastic wave equations, bulletin of the Seismological Society of America, **67**, 1529-1540.

Engquist, B. and Majda, A., Absorbing boundary conditions for numerical simulation of waves, Proc. Natl. Acad. Sci. USA, 74, 1765-1766.

Gavrilov, D., Lines, L., Bland, H., Kocurko, A., 2000, 3-D depth migration: parallel processing and migration movies, The Leading Edge, **19**, 1282-1284.

Jiang, Z., Bancroft, J.C., and Lines, L.R., 2010, Combining absorbing and nonreflecting boundary conditions for elastic wave simulation, SEG International Exposition and Eightieth Annual Meeting, Denver, Colorado.

Jiang, Z., Bonham, K., Bancroft, J.C., and Lines, L.R., 2010, Overcoming computational cost problems of reverse-time migration, GeoCanada 2010 Conference

Jiang, Z., Bancroft, J.C., Lines, L.R., and Hall, K.W., 2010, Elastic prestack reverse-time migration using a staggered-grid finite-difference method, GeoCanada 2010 Conference

Kaelin B., and Guitton A., 2006, Imaging condition for reverse time migration, SEG/New Orleans 2006 annual meeting, 2594-2598.

Loewenthal, D., and Hu, L., 1991, Two methods for computing the imaging condition for common-shot prestack migration: Geophysics, **56**, 378–381.

Manning, P.M., 2008, Techniques to enhance the accuracy and efficiency of finite-difference modeling for the propagation of elastic waves, PhD thesis, University of Calgary.

Martin, G.S., 2004, The marmousi2 model, elastic synthetic data, and an analysis of imaging and AVO in a structurally complex environment, MSc thesis, University of Houston.

Virieux, J., 1986. P-SV wave propagation in heterogeneous media: velocity-stress finite-difference method, Geophysics, **51**, 889--901.

Whitmore, N.D., and Lines, L.R., 1986, Vertical seismic profiling depth migration of a salt dome flank: Geophysics, **51**, 1087-1109.